# Track Registration in Various Solid-State Nuclear Track Detectors

R. L. FLEISCHER, P. B. PRICE, AND R. M. WALKER
*General Electric Research Laboratory, Schenectady, New York*

AND

E. L. HUBBARD
*Lawrence Radiation Laboratory, University of California, Berkeley, California*

(Received 23 September 1963)

In a number of materials energetic, heavy nuclear particles leave trails of radiation-damaged material which can be selectively attacked by chemical reagents to produce tracks visible in the optical microscope. The track-registration characteristics of three such materials—muscovite mica, Lexan polycarbonate, and cellulose nitrate—were investigated using fission fragments and various heavy ions from argon down to helium, each over a wide range of energies. Curves of energy-loss rate $dE/dx$ versus particle energy were calculated for each solid, and the experimental results were displayed on the $dE/dx$ curves. It was found that for each detector there is a fairly narrow range of $dE/dx$ values over which the track-registration efficiency varies from unity to zero. This rapid drop in efficiency with $dE/dx$ makes it reasonable to define a critical energy-loss rate $(dE/dx)_{\text{crit}}$ for each detector, which appears to be independent of energy and atomic number. Crude estimates of particle masses can be made using several detectors with different $(dE/dx)_{\text{crit}}$. For example, for particles with energies less than $\sim$3 MeV/amu, the mass must exceed 3, 12, and 28 amu if tracks register in cellulose nitrate, Lexan polycarbonate, and muscovite, respectively. For particles such as fission fragments, with initial $dE/dx \gg (dE/dx)_{\text{crit}}$, the track lengths are a fair approximation of the particle ranges. Particles incident at a very small angle to a detector surface are registered in mica but not in plastics or glasses. Solid-state track detectors presently offer unique advantages when heavy particles must be studied in the presence of a high background flux of light particles.

## I. INTRODUCTION

A NEW class of detectors for the visual study of charged nuclear particle trajectories has been developed within the past year or so. We choose to call them solid-state nuclear track detectors, and we exclude from this category nuclear emulsions because of fundamental differences in structure and track development technique.

The new detectors are initially homogeneous in structure. A detector may be a single crystal such as mica[1] or AgBr,[2] or a homogeneous noncrystalline solid such as an inorganic glass[3] or a high polymer.[4] In principle there is no limitation on size or shape, and in fact it may be thin enough for tracks to be viewed in an electron microscope, thus giving extremely high spatial resolution.[5]

Charged particles which impinge on a solid-state nuclear track detector locally alter its structure, either by ionization processes or by colliding with atoms and ejecting them from their proper positions. Under certain conditions to be considered below, the resulting radiation-damaged regions may be nearly continuous along the particle trajectories and can be developed to a convenient size for viewing in an optical microscope.

Two development techniques have been employed: (1) Metal ions in a transparent solid may be reduced and precipitated preferentially along the damaged regions, giving rise to opaque tracks.[2,3] (2) The solid may be chemically etched in a reagent which attacks primarily the damaged regions whose structure and chemical reactivity have been altered. Fine channels are thus produced which accurately delineate the particle trajectories and which show up as dark tracks if the solid is transparent and is viewed by transmitted light.

The second technique is by far the more general one. The differential etching effect has been demonstrated in homogeneous, electrically insulating solids of many different types—ionic crystals,[6,7] covalent crystals,[7] layer-structure crystals,[8] glasses,[3] and plastics.[4]

Solid-state track detectors have several advantages over conventional detectors in certain experiments involving particle detection. Their effectiveness has already been demonstrated in studies of geochronology,[9–12] in neutron dosimetry,[13] and in studies of the fission of heavy nuclei,[14,15] and they are currently being employed in a variety of other experiments.

In order to utilize the various detectors properly, it is essential to know their track-registration characteristics.

[1] P. B. Price and R. M. Walker, Phys. Letters **3**, 113 (1962).
[2] C. Childs and L. Slifkin, IRE Trans. Nucl. Sci. **9**, 143 (1962).
[3] R. L. Fleischer and P. B. Price, J. Appl. Phys. **34**, 2903 (1963).
[4] R. L. Fleischer and P. B. Price, Science **140**, 1221 (1963).
[5] P. B. Price and R. M. Walker, Phys. Rev. Letters **8**, 217 (1962).
[6] D. A. Young, Nature **182**, 375 (1958).
[7] R. L. Fleischer and P. B. Price (unpublished results).
[8] P. B. Price and R. M. Walker, J. Appl. Phys. **33**, 3407 (1962).
[9] P. B. Price and R. M. Walker, J. Geophys. Res. **68**, 4847 (1963).
[10] R. L. Fleischer and P. B. Price, J. Geophys. Res. **69**, 331 (1964).
[11] M. Maurette, P. Pellas, and R. M. Walker, Bull. Soc. Franc. Miner. Crist. (to be published).
[12] R. L. Fleischer, D. S. Miller, P. B. Price, and E. M. Symes, Science (to be published).
[13] R. M. Walker, P. B. Price, and R. L. Fleischer, Appl. Phys. Letters **3**, 28 (1963).
[14] P. B. Price, R. L. Fleischer, R. M. Walker, and E. L. Hubbard, in *Proceedings of the Conference on Reactions between Complex Nuclei* (University of California Press, 1963); also as University of California, Lawrence Radiation Laboratory Report No. UCRL-10772 (1963).
[15] D. S. Burnett, F. Placil, P. B. Price, W. J. Swiatecki, and S. G. Thompson, Phys. Rev. (to be published).

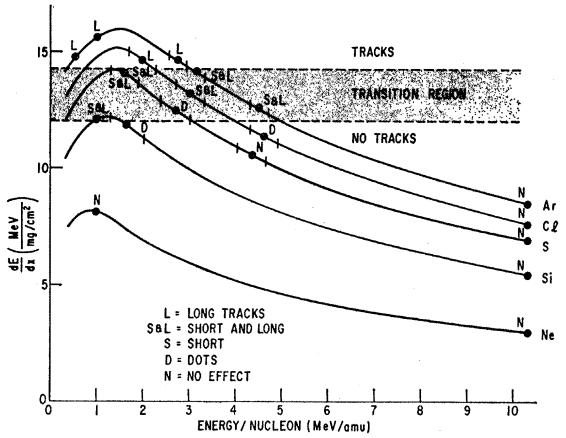


FIG. 1. Track registration in muscovite mica. The curves show the calculated rates of energy loss of various heavy ions in mica as a function of energy per nucleon. The track-registration efficiency increases from 0 to 100% within the shaded band marked "transition region" in the figure, and the average track length increases from 0 to full length. There is thus a fairly well-defined critical rate of energy loss for track production which appears to be independent of energy. Impinging particles lighter than Si are not detected and do not impair the ability of mica to detect heavier particles.

The main purpose of this paper is to provide this information for three different solids—muscovite mica, Lexan polycarbonate resin, and cellulose nitrate—which have markedly different track-registration characteristics. To do this we have exposed these detectors to known doses of a wide variety of particles ranging in mass from fission fragments down to alpha particles, each over a wide range of energies. We have then made quantitative microscopic studies of the tracks formed by the various particles.

## II. THE CONCEPT OF A CRITICAL RATE OF ENERGY LOSS FOR TRACK FORMATION

In conventional track-registering devices—cloud chambers, bubble chambers, and nuclear emulsions—the linear density of droplets, bubbles, or silver halide grains is a function of the rate of energy loss of the charged particle by electronic excitation and ionization. Initial experiments[1,5,8] in which mica was bombarded with several types of particles suggested that $dE/dx$, the average rate of energy loss of the particle in the solid, might also be the relevant parameter which determines whether a track can be chemically etched in a solid-state detector.

The present work confirms the validity of the concept of a threshold value of $dE/dx$ for track production and shows that $(dE/dx)_{\text{crit}}$ varies from solid to solid.

We first calculate curves of $dE/dx$ as a function of energy per nucleon for various heavy ions in three useful solid-state track detectors—muscovite mica, Lexan polycarbonate, and cellulose nitrate. We then tabulate the results of track-registration experiments. When the data are displayed on the $dE/dx$ curves, it will be seen that for each detector there is a fairly narrow range of $dE/dx$ values where the track-registration efficiency varies from unity to zero. This rapid change of efficiency over a narrow range of $dE/dx$ values makes it reasonable to define a critical rate of energy loss $(dE/dx)_{\text{crit}}$ for each detector.

The $dE/dx$ curves, shown in Figs. 1 and 2, are calculated in the following way: The rate of energy loss of a charged particle with a given velocity $\beta=v/c$ can be related to the rate of energy loss of a proton with the same velocity through the equation

$$\left(\frac{dE}{dx}\text{ion}\right)_{\beta}=[z^*(\beta)]^2\left(\frac{dE_p}{dx}\right)_{\beta}, \tag{1}$$

which defines an "effective charge" $z^*$ of the particle.[16] We need to know both $z^*(\beta)$ and $(dE_p/dx)_\beta$. In Fig. 7 of their paper, Heckman *et al.*[16] have plotted values of $z^*/z$ as a function of $\beta/z^{2/3}$, where $z$ is the nuclear charge, using their heavy-ion data and other published data compiled by Whaling.[17] The experimental points follow a "universal curve" which we have used to calculate values of $z^*$ for various ions and velocities.

Proton-energy-loss rates have been measured in muscovite only for energies less than 2 MeV,[18] and no energy-loss data exist for Lexan polycarbonate or cellulose nitrate. We have supplemented the energy-loss data in muscovite by calculating $dE_p/dx$ for energies between 2 and 10 MeV and have also calculated $dE_p/dx$ in the two polymers from 1 to 10 MeV by utilizing the approximately additive relationship between the molecular stopping cross section $\epsilon_{\text{mol}}$ of a compound and the atomic stopping cross sections of the constituent atoms[18]:

$$\epsilon_{\text{mol}}(X_nY_m)=n\epsilon(X)_{\text{at}}+m\epsilon(Y)_{\text{at}}. \tag{2}$$

The rate of energy loss of a proton in the compound is then $dE_p/dx=-N\epsilon_{\text{mol}}(X_nY_m)$, where $N$ is the number

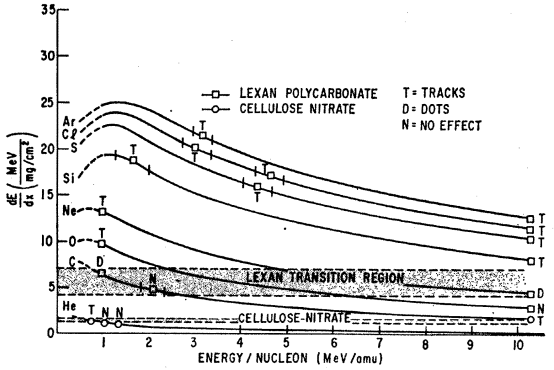


FIG. 2. Track registration in two polymers with different critical rates of energy loss. Lexan polycarbonate can detect low-energy oxygen ions and cellulose nitrate can even detect low-energy alpha particles. Above the transition regions the track lengths increase with $dE/dx$ and are therefore not reliable indicators of particle range.

[17] W. Whaling, in *Handbuch der Physik*, edited by S. Flügge (Springer-Verlag, Berlin, 1958), Vol. 34, p. 193.
[18] S. K. Allison and S. D. Warshaw, Rev. Mod. Phys. **25**, 779 (1953).

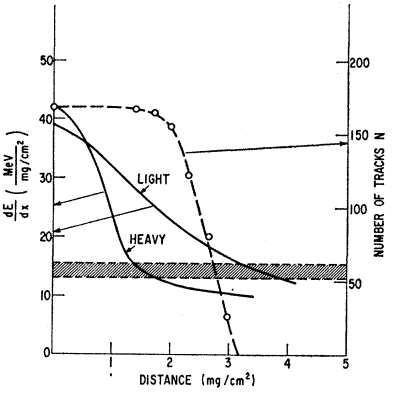


FIG. 3. Estimated curves of energy-loss rates of light ($Z=38$, $A=95$) and heavy ($Z=54$, $A=139$) fission fragments in Al. The shaded horizontal band represents the transition region for track detection in mica. The dashed line is obtained from the experimentally measured distribution of track lengths in mica (Fig. 5) and represents the number of tracks with a length greater than the value of the abscissa.

of molecules per gram. Using the empirical formulas for atomic stopping cross sections of various elements tabulated by Whaling,[18] the equations for $dE_p/dx$ in muscovite ($KAl_3Si_3O_{12}H_2$), Lexan polycarbonate (approximately $H_{18}C_{16}O_3$), and cellulose nitrate ($H_6C_{12}O_{18}N_4$) are

$$\left(\frac{dE_p}{dx}\right)\text{muscovite}=\left[0.060\frac{\ln E_p}{E_p}+\frac{0.164}{E_p}\right]\frac{\text{MeV}}{\text{mg/cm}^2},$$

$$\left(\frac{dE_p}{dx}\right)\text{Lexan polycarbonate}=\left[0.077\frac{\ln E_p}{E_p}+\frac{0.266}{E_p}\right]\frac{\text{MeV}}{\text{mg/cm}^2}, \quad (3)$$

$$\left(\frac{dE_p}{dx}\right)\text{cell. nitrate}=\left[0.073\frac{\ln E_p}{E_p}+\frac{0.232}{E_p}\right]\frac{\text{MeV}}{\text{mg/cm}^2},$$

with $E_p$ given in MeV. The calculated value of $dE_p/dx$ in muscovite for $E_p=2$ MeV was in good agreement with the experimentally measured value,[18] so that the curve of $dE_p/dx$ versus $E_p$ in muscovite varies smoothly from 0.35 to 10 MeV.

The rate of energy loss of a given ion with velocity $\beta$ is then given by (1), with $z^*(\beta)$ read from Fig. 7 of Heckman's paper[16] and $(dE_p/dx)_\beta$ calculated from the appropriate equation in (3) and from the experimental proton-energy-loss data for muscovite below $E_p=2$ MeV. Energy-loss curves for muscovite are plotted in Fig. 1 for Ar, Cl, S, Si, and Ne ions between 0.35 and 10 MeV/nucleon. The curves for Lexan polycarbonate and cellulose nitrate are not significantly different, so that a single set of curves, applicable to both polymers within the uncertainties in the calculations, is plotted in Fig. 2 for Ar, Cl, S, Si, Ne, O, C, and He between 1 and 10 MeV/nucleon.

It is difficult to obtain accurate $dE/dx$ curves for fission fragments in the various detectors. Accurate range-energy data exist only for median-mass heavy fragments ($Z=54$, $A=139$) and median-mass light fragments ($Z=38$, $A=95$) from thermal fission of $U^{235}$. We have graphically differentiated Fulmer's[19] curves for fission fragments in aluminum, whose stopping power for heavy ions is within 10% of that of mica. The resulting curves, shown in Fig. 3, are useful for qualitatively understanding the fission-fragment registration data presented in the following section.

## III. EXPERIMENTAL MEASUREMENTS OF TRACK-REGISTRATION EFFICIENCY

### 1. Heavy Ions and Alpha Particles

Thin slabs of mica, Lexan polycarbonate, and cellulose nitrate were mounted on aluminum wedges and bombarded at a 30° angle with known doses of various particles in the Berkeley heavy ion accelerator,[20] which can accelerate ions of a number of elements up to a maximum energy of 10.4 MeV/nucleon. Other accurately known energies, 0.11 and 0.97 MeV/nucleon, were obtained by using only the Cockroft-Walton injector and by using the Cockroft-Walton and prestripper accelerator. Bombardments at other energies were performed by using accurately weighed Al degrader foils and calculating the energies from tabulated range-energy data.[21]

The ion beam was defocused so as to irradiate the detectors uniformly. Each wedge was screwed into a Faraday cup, which was calibrated (for all but the earliest runs) to read the integrated dose to within ~10%.

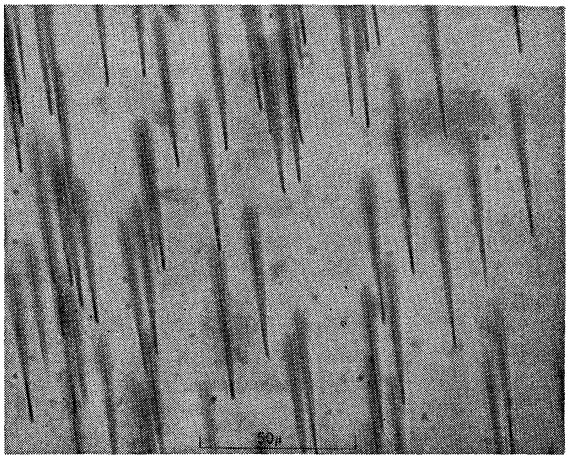

FIG. 4. Etched tracks of 139-MeV $S^{32}$ ions entering Lexan polycarbonate at a 30° angle. The average track length is ~53 $\mu$, whereas the true range of the ions is estimated to be 60 $\mu$. The micrograph was taken by transmitted light with the microscope focused below the surface on the ends of the tracks.

[19] C. B. Fulmer, Phys. Rev. **108**, 1113 (1957).
[20] E. L. Hubbard, Rev. Sci. Instr. **32**, 621 (1961).
[21] E. L. Hubbard, University of California, Lawrence Radiation Laboratory Report No. UCRL-9053, 1960 (unpublished).

TABLE I. Track registration in various detectors.

| Ion | Energy (MeV) | Dose ($cm^{-2}$) | Track density ($cm^{-2}$) | Length variation ($\mu$) | Observing technique[a] |
|---|---|---|---|---|---|
| | | | Muscovite mica | | |
| $Ar^{40}$ | 414 ± 5 | $\sim 1.5\times10^{12}$ | $\sim10^{8}$ background[b] | 0 | e.m. |
| $Ar^{40}$ | 180 ± 5 | $(1.5\pm0.2)\times10^{8}$ | $(1.5\pm0.5)\times10^{8}$ | 0 to 8 (mainly dots)[c] | e.m. |
| $Ar^{40}$ | 125 ± 8 | $(3.1\pm1.0)\times10^{7}$ | $(3\pm1)\times10^{7}$ | $\sim$0 to $\sim$8 | o.m. |
| $Ar^{40}$ | 110 ± 8 | $\sim10^{8}$ | $(1.7\pm0.3)\times10^{8}$ | $\sim$25 | e.m., o.m. |
| $Ar^{40}$ | 38.8 ± 0.7 | $(3.2\pm1.0)\times10^{8}$ | $(6\pm4)\times10^{8}$ | long[c] | e.m. |
| $Ar^{40}$ | 20 ± 3 | $(1.2\pm0.2)\times10^{9}$ | $(0.9\pm0.4)\times10^{9}$ | long[c] | e.m. |
| $Ar^{40}$ | 4.4 ± 0.1 | $(5.9\pm2.0)\times10^{7}$ | $\sim5\times10^{6}$ | $\sim$0 to 0.5 | e.m. |
| $Cl^{35}$ | 363 ± 4 | $(3.9\pm0.4)\times10^{6}$ | $\sim10^{3}$ background[b] | 0 | o.m. |
| $Cl^{35}$ | 161 ±10 | $(3.5\pm0.5)\times10^{6}$ | $(2.2\pm0.3)\times10^{6}$ | $\sim$0 (dots) | o.m. |
| $Cl^{35}$ | 105 ±10 | $(3.0\pm0.4)\times10^{6}$ | $(2.8\pm0.2)\times10^{6}$ | $\sim$0 to $\sim$14 | o.m. |
| $C^{35}$ | 69 ±10 | $(4.4\pm0.6)\times10^{6}$ | $(5.3\pm0.2)\times10^{6}$ | $\sim$6 to $\sim$10 | o.m. |
| $S^{32}$ | 331 ± 4 | $\sim2\times10^{11}$ | $10^{7}$–$10^{8}$ background[b] | 0 | o.m. |
| $S^{32}$ | 139 ±10 | $(3.1\pm0.4)\times10^{6}$ | $\sim10^{2}$–$10^{3}$ background[b] | 0 | o.m. |
| $S^{32}$ | 86 ±10 | $(5.6\pm0.7)\times10^{6}$ | $(2.3\pm0.3)\times10^{6}$ | $\sim$0 (dots) | o.m. |
| $S^{32}$ | 51 ±10 | $(5.3\pm0.7)\times10^{6}$ | $(4.6\pm0.3)\times10^{6}$ | $\sim$1 to 10 | o.m. |
| $Si^{28}$ | 46 ±10 | $(2.2\pm0.3)\times10^{7}$ | $(8\pm4)\times10^{6}$ | $\sim$0 (dots) | o.m. |
| $Si^{28}$ | 27.2 ± 0.5 | $(1.05\pm0.1)\times10^{8}$ | $(5.6\pm0.7)\times10^{7}$ | $\sim$0 to 5 | o.m. |
| $Ne^{20}$ | 19.4 ± 0.2 | $(2.4\pm0.4)\times10^{8}$ | $\sim10^{3}$ background dots[b] | 0 | o.m. |
| | | | Lexan polycarbonate | | |
| $Ar^{40}$ | 125 ± 8 | $(3.1\pm1.0)\times10^{7}$ | $(3.8\pm0.4)\times10^{7}$ | $\sim$40 to $\sim$45 | o.m. |
| $Cl^{35}$ | 363 ± 4 | $(3.9\pm0.4)\times10^{6}$ | $(5\pm0.5)\times10^{6}$ | $\sim$2 to 6 | o.m. |
| $Cl^{35}$ | 105 ±10 | $(3.0\pm0.4)\times10^{6}$ | $(3.6\pm0.4)\times10^{6}$ | $\sim$30 to 35 | o.m. |
| $Cl^{35}$ | 161 ±10 | $(3.5\pm0.5)\times10^{6}$ | $(3.4\pm0.3)\times10^{6}$ | $\sim$23 to 28 | o.m. |
| $S^{32}$ | 139 ±10 | $(3.1\pm0.4)\times10^{6}$ | $(3.3\pm0.3)\times10^{6}$ | $\sim$50 to 55 | o.m. |
| $Si^{28}$ | 290 ± 3 | $(2.0\pm0.3)\times10^{7}$ | $(2.1\pm0.05)\times10^{7}$ | $\sim$3 to $\sim$7 | o.m. |
| $Si^{28}$ | 46 ±10 | $(2.2\pm0.3)\times10^{7}$ | $(1.7\pm0.1)\times10^{7}$ | $\sim$4 to $\sim$8.5 | o.m. |
| $Ne^{20}$ | 207 ± 3 | $(9.7\pm0.9)\times10^{7}$ | $(6\pm2)\times10^{7}$ | $\sim$0 to 1.5 | o.m. |
| $Ne^{20}$ | 19.4 ± 0.2 | $(2.4\pm0.4)\times10^{8}$ | too dense to measure | $\sim$2 to 4 | o.m. |
| $O^{16}$ | 166 ± 2 | $(9.3\pm0.8)\times10^{6}$ | 0 | 0 | o.m. |
| $O^{16}$ | 15.5 ± 0.2 | $(1.7\pm0.2)\times10^{8}$ | too dense to measure | $\sim$0.5 to 1.5 | o.m. |
| $C^{12}$ | 25 ± 3 | $(1.1\pm0.1)\times10^{7}$ | 0 | 0 | o.m. |
| $C^{12}$ | 11.65± 0.2 | $(2.6\pm0.3)\times10^{7}$ | varying with position | $\sim$0 to 1 | o.m. |
| $He^{4}$ | $\sim$1 to 5.45 | $\sim10^{8}$ | 0 | 0 | o.m. |
| | | | Cellulose nitrate | | |
| $O^{16}$ | 166 ± 2 | $(9.3\pm0.8)\times10^{6}$ | $(5\pm3)\times10^{6}$ | >10 | o.m. |
| $C^{12}$ | 124 ± 2 | $(1.2\pm0.1)\times10^{7}$ | $(9\pm2)\times10^{6}$ | $\sim$5 | o.m. |
| $He^{4}$ | 5.45 | $(2.5\pm0.5)\times10^{6}$ | 0 | 0 | o.m. |
| $He^{4}$ | 4.18 | $(5\pm1)\times10^{4}$ | 0 | 0 | o.m. |
| $He^{4}$ | 3 ± 1 | $\sim10^{8}$ | $\sim10^{8}$ | $\sim$3 to 6 | o.m. |

[a] e.m., electron microscope; o.m., optical microscope.
[b] The low density of background tracks in 10.4-MeV/nucleon Hilac beams is attributed to ions with the same magnetic rigidity but a higher $dE/dx$ than the nominal ions.
[c] Electron-microscope specimens are typically less than 0.5 $\mu$ thick, so that only the initial portion of a track can be seen and the full length cannot be measured.

Normally doses of $\sim10^{6}$ to $10^{8}$ ions/cm$^{2}$ were employed. In some of the argon runs, very thin samples were exposed to high doses and then examined in an electron microscope, particularly when low-energy, short-range ions were used.

The following bottled chemicals were used as ion sources: argon gas, $CCl_4$ (for chlorine), $H_2S$ (for sulfur), $SiF_4$ (for silicon), neon gas, oxygen gas, and $CO_2$ (for carbon). The proper isotopes and charge states were selected magnetically.

$Am^{241}$ and $Po^{210}$ films, together with accurately weighed Al foils of various thicknesses, were employed as sources of alpha particles with energies up to 5.48 MeV.

Information on specimen preparation and etching data is presented in the Appendix.

Figure 4 is a photomicrograph showing etched heavy-ion tracks in Lexan polycarbonate. In Table I are listed the ions, bombarding energies, doses, measured track densities, appearance of the tracks, and the observing instrument (optical or electron microscope). The relationship between the qualitative appearance of the tracks and $dE/dx$ can be easily visualized by referring to Figs. 1 and 2 and their legends.

## 2. Fission Fragments

Mica, Lexan polycarbonate, and cellulose nitrate were irradiated with well-collimated fragments from the spontaneous fission of $Cf^{252}$. The source, a very thin film ($\sim10^{-8}$ g) of $Cf^{252}$ on a Pt substrate, was covered with an Al disk containing a 0.5-mm pinhole. The space between the Cf and the detectors was evacuated so that fragments entered the targets with nearly their original kinetic energy. The position of the targets could be adjusted so that fission fragments entered the surface

at any desired angle. Two experiments were done:

(1) The detectors were bombarded with known doses at a fixed angle of 20°, and the number of tracks as a function of length was measured. The resulting track-length distributions are plotted in Fig. 5. For each material the optimum etching times (see Appendix) for producing the longest tracks were used. In addition, for mica the number of tracks exceeding a certain length, as a function of length, is plotted in Fig. 3 for comparison with the $dE/dx$ curves in Al of light and heavy fragments from the thermal fission of $U^{235}$.

(2) Because the surfaces of some detectors dissolve at a finite rate during etching, tracks incident at a very shallow angle in these detectors will not be detectable.[10] It has previously been established that the cleavage plane surfaces of mica do not dissolve and that the registration efficiency is independent of angle.[8] Using the $Cf^{252}$ source, Lexan polycarbonate and cellulose nitrate were bombarded at various angles from 30° down to ~4°. In Lexan polycarbonate, fission fragments were recorded independently of angle down to 4°, whereas in cellulose nitrate a critical angle of ~4° was found, below which the surface was dissolved faster than the track material was etched out. This difference is treated in Sec. IV. 3.

## IV. DISCUSSION

### 1. Dependence of Track Registration on $dE/dx$

In these experiments we have chosen bombarding particles of different energies and masses in order to study the registration of particle tracks as a function of the quantity $dE/dx$. Provided the initial energy of the particle is sufficiently high, $dE/dx$ remains approximately constant for a penetration distance equal to the minimum distance $x_{\min}$ necessary to form a recognizable track. For optical observation, $x_{\min} \approx 1.5$ to $2\,\mu$. The track-registration efficiency at a given $dE/dx$ is then the fraction of particles which enter the detector with this initial $dE/dx$ and form "observable tracks," i.e., tracks whose lengths are at least as great as $x_{\min}$.

The results show that for high-energy particles with large $dE/dx$ values, the efficiency is unity. The track lengths are uniformly much longer than $x_{\min}$ and are of the order of the actual range of the particles in the medium. As particles are chosen, however, which have lower and lower $dE/dx$ values, the registration efficiencies suddenly drop and the average track lengths shorten, becoming much less than the known range of the particles in the medium. At sufficiently low $dE/dx$ rates the efficiency drops to zero, and no tracks are observed.

In Figs. 1 and 2 we have drawn a shaded region for each detector corresponding to this transition region between complete and zero registration. As can be seen be referring to the figures, below the upper boundaries the tracks begin to be imperfectly formed, sometimes giving only small dots instead of real tracks, whereas below the lower boundaries no observable tracks are formed.

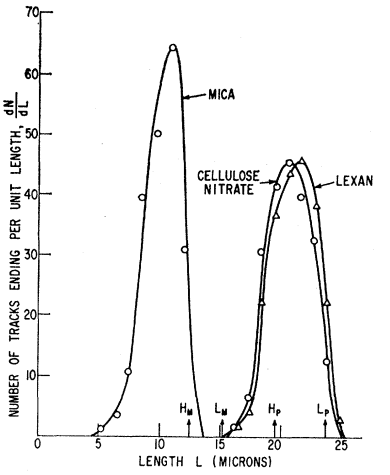


FIG. 5. Length distributions of fragments from the spontaneous fission of $Cf^{252}$, which have impinged at a 20° angle on three detectors. The arrows along the abscissa indicate the estimated ranges of light ($Z=38$, $A=95$) and heavy ($Z=54$, $A=139$) fragments in mica ($L_M$, $H_M$) and in the polymers ($L_p$, $H_p$).

In mica the transition region is remarkably sharp, and the detection efficiency drops from 100% to zero with a decrease in $dE/dx$ of less than 20%. The critical $dE/dx$ is thus well defined and appears to be a constant, independent of energy and the type of bombarding particle. Fewer experimental points were obtained for the polymers, so that in this case one cannot with certainty say that $(dE/dx)_{\text{crit}}$ has been shown to be the determining parameter independent of particle type and energy. In particular, Lexan polycarbonate appears to register high-energy neon ions with a lower $dE/dx$ than low-energy carbon ions, which are not registered. The caluclated $dE/dx$ curves for the polymers are rather uncertain at energies less than 2 MeV/nucleon, and this may account for the discrepancy.

### 2. Measurement of Particle Ranges

The quantity $dE/dx$ is a double-valued function of particle energy as can be seen by referring to the curves of Figs. 1 and 2. If a particle enters the detector with an energy greater than that corresponding to the maximum in $dE/dx$, then as the particle slows down its $dE/dx$ value should first increase, reach a maximum, and then decrease again towards the very end of the particle range. If the initial value of $dE/dx$ is considerably above the critical value, all of the particle path except the very last bit should be attacked during etching, and the track length should closely approximate the range of the particle.

In mica $(dE/dx)_{\text{crit}}$ is so high that in only four of the exposures listed in Table I were ions expected to register with 100% efficiency. In two of the exposures (38.8- and 20-MeV Ar ions) the full tracks were not observed because the electron microscope was used. The other

two exposures, to 110-MeV Ar and 96-MeV Cl, produced etched tracks $\sim 25\,\mu$ long and up to $\sim 10\,\mu$ long, respectively. From calculated heavy-ion range-energy curves[21] we conclude that these track lengths are about equal to the distances traveled by the ions before their $dE/dx$ dropped below $(dE/dx)_{\text{crit}}$.

In the polymers the etching rate along a track is an increasing function of $dE/dx$ even above $(dE/dx)_{\text{crit}}$, i.e., the more severe the radiation damage the greater the chemical reactivity along the track. Only when $dE/dx$ remains well above the threshold value does the track length closely approximate the particle range. Thus, after the standard etching time for Lexan polycarbonate, tracks of 10-MeV/amu ions of Ar, Cl, S, Si, and Ne are only a few microns long and decrease with decreasing $dE/dx$, even though they register with 100% efficiency and though the calculated particle ranges are well over $100\,\mu$ for each ion. It is only for the low energy Ar, Cl, and S ions (and for full-energy fission fragments) that the track lengths approach the calculated ion ranges.

Let us now consider the fission-fragment results. If we represent the spectrum of fragment masses by equal numbers of particles of mass 139 and 95, then in mica we expect the registration efficiency to decrease beyond the range at which $dE/dx$ for the heavy fragment reaches $(dE/dx)_{\text{crit}}$. At the distance where $dE/dx$ for the light fragment has also dropped to $(dE/dx)_{\text{crit}}$, no tracks should be observed. The curve of observed track density vs distance traveled in mica (Fig. 3) does just this, and the track density has dropped to zero before the end of the calculated range of either fragment. Since the ranges of fission fragments are difficult to calculate exactly, this cannot be taken as a definitive, independent proof of the validity of the $(dE/dx)_{\text{crit}}$ hypothesis, but the results are certainly consistent with this view.

In the two polymers studied, the thresholds for particle detection are so low that fission fragments should be observed over essentially their entire range. On the basis of the assumption of two unique particles, light and heavy, we estimate from measured range-energy curves of heavy ions in plastics[22] that two separated peaks corresponding to $\sim 19.5$ and $\sim 24\,\mu$ should be observed in Lexan polycarbonate and cellulose nitrate. Actually, the measured length distributions in these polymers give a single peak at $\sim 21$ to $22\,\mu$. It should be remembered, however, that there are a range of masses and energies for the fission fragments and that this tends to merge the individual range peaks into a single peak.

In a photographic-emulsion study, Vigneron[23] was able to resolve the two types of particles, but the statistics in that experiment were such that a single peak cannot be excluded.

In an indepencent study, generally corroborating the present work, Debeauvais *et al.*[24] compared $U^{235}$ fission-fragment tracks in mica, Lexan polycarbonate, and photographic emulsions. The photographic-emulsion length distribution gave a single peak and this, coupled with the close agreement on the calculated and measured ranges of the fragments in the plastics, allows one to conclude that, within a maximum error of 10%, the measured track lengths correspond to the actual ranges in plastic.

It is of course possible that towards the very end of the range the fission fragments are not registered or are registered imperfectly. The only measurement of registration efficiency at very low energy was the electron-microscope observation of tracks of 4-MeV Ar ions, which appears to be compatible with the other data. A low efficiency ($\sim 10\%$) and a predominance of pits rather than tracks implies that $dE/dx$ is less than the threshold value. Unfortunately, the $dE/dx$ curves are not known below 0.35 MeV/nucleon.

The extension of track-registration data to very low energies by electron microscopy would be of great interest because the mechanism of energy loss is predominantly by atomic collisions rather than by electronic excitation and ionization. The question of registration of low-energy particles is of no concern in optical-microscope studies of tracks because the ranges are unresolvably small.

### 3. Dependence of Track Registration on Angle of Entry

Most detector materials (an exception being mica) dissolve uniformly on all exposed surfaces with a velocity $v_G$ which must be much smaller than the rate of attack along a track $v_T$ in order for the tracks to define particle trajectories.[3,4] In these materials tracks are narrow cones whose half-angle is $\arcsin(v_G/v_T)$. If a track meets a surface at an angle less than $\theta_c \equiv \arcsin(v_G/v_T)$, the rate of dissolution of the surface exceeds the component of $v_T$ normal to the surface, and no track can be formed.

Since the cleavage planes of mica are not attacked by hydrofluoric acid, tracks at all angles should be revealed, and this was found experimentally to be the case. In cellulose nitrate $\theta_c$ was found to be $\sim 4°$, and in Lexan polycarbonate $\theta_c$ was shown to be less than 4°. In initial studies of Lexan polycarbonate, $v_G$ and $v_T$ were measured, from which we would deduce $\theta_c \leq \arcsin 0.05 = 2.9°$. One should therefore be cognizant in using these plastics that particles incident at very small angles will not be detected.

In most glasses $\theta_c$ is so large that they are unsuitable for most applications as solid-state track detectors. In soda-lime glass,[25] $\theta_c \approx 30°$; in silica,[10] $\theta_c \approx 17°$; and in phosphate glasses,[3] $\theta_c$ is usually $\sim 8°$.

[22] P. E. Schambra, A. M. Rauth, and L. C. Northcliffe, Phys. Rev. **120**, 1758 (1960).

[23] L. Vigneron, Compt. Rend. **231**, 1473 (1950).

[24] M. Debeauvais, M. Maurette, J. Mory, and R. M. Walker, J. Appl. Rad. Isotopes (to be published).

[25] R. L. Fleischer and P. B. Price (unpublished results).

### 4. Particle Identification

The main advantages of solid-state track detectors over conventional devices are their simplicity and their complete insensitivity to particles with $dE/dx$ below threshold. In addition, it should be possible by using several detectors with different values of $(dE/dx)_{crit}$ to make crude estimates of particle identities. For example, using the three detectors described in this paper, if the particles in question are known to have rather low energies (less than ~3 MeV/amu), the mass must be greater than 3 or 4 if tracks show up in cellulose nitrate, greater than ~12 if tracks appear in Lexan polycarbonate, and greater than ~28 if tracks appear in mica.

If the particles are known to have extremely high energies (e.g., cosmic rays), the minimum values for their atomic numbers are estimated to be ~27, 72, and 120 for tracks in cellulose nitrate, Lexan polycarbonate, and mica, respectively. These estimates were made by taking $dE/dx = 10^{-3}$ MeV/(mg/cm$^2$) for minimum ionizing singly charged particles in nuclear emulsion[26] and finding what atomic number a heavy particle with the same velocity would have in order to be losing energy at the critical rate for the detector in question.

Nuclear-emulsion techniques are sufficiently advanced that particles can usually be identified within one or two units of $Z$. In the presence of a large background of light particles, however, the emulsion technique eventually breaks down, and it is under these conditions that solid-state track detectors may offer unique advantages. Many classes of polymers have been found which exhibit the particle etching effect, and it is likely that a family of detectors with values of $(dE/dx)_{crit}$ spanning the gaps between mica, Lexan polycarbonate, and cellulose nitrate can eventually be classified. It is also not unreasonable to expect that more sensitive materials than cellulose nitrate will be found.

#### ACKNOWLEDGMENTS

One of us (P.B.P.) is pleased to acknowledge the hospitality of S. G. Thompson and the Lawrence Radiation Laboratory during part of this work. We are also indebted to S. G. Thompson for his generous loan of the calibrated $Cf^{252}$ source.

#### APPENDIX

### 1. Detector Preparation

High-quality muscovite mica can be obtained from any mineral supplier. It normally contains tracks resulting from the spontaneous fission of uranium impurities over geologic times.[9] The density of such background tracks ranges from a few up to perhaps $10^4$ per cm$^2$ of freshly cleaved surface. In order to avoid confusion, one selects a mica with a low background and then etches it for a sufficiently long time such that the tracks are holes too large to be confused with deliberately induced tracks. No other preparation is necessary. If synthetic mica is used, even this step can be omitted, since it is not old enough to contain "fossil" tracks.

Polycarbonate resin (Plestar) which is similar to Lexan polycarbonate can be bought in a convenient roll 35 mm wide and 0.004 in. thick: Ansco, Plestar base unsubbed, 17-386 unperforated. Thin films suitable for electron-microscopic study can be made by pouring onto a water surface a drop of a methylene dichloride solution containing Lexan polycarbonate resin, grade 105 or 125 (G.E. Chemical Materials Department, Pittsfield, Massachusetts). The solvent evaporates, leaving a thin film which can be picked up on a wire ring.

Sheets or films of cellulose nitrate can be made in a similar way by pouring onto a smooth surface a solution of amyl acetate containing nitrocellulose. After the solvent evaporates, the film or sheet *must be annealed* at a temperature of ~50 to 100°C in order to drive out residual solvent. If this is not done, cone-shaped pits instead of more uniform tracks will result from etching (see, e.g., Fig. 2 in Ref. 4).

### 2. Etching Conditions

Curves of track diameters in various types of mica as a function of etching time have been reported for 20% HF at room temperature and at 50°C.[8] In micas the acid very rapidly permeates the continuously damaged portion of a particle trajectory and then begins to dissolve the surrounding material, attacking only in a direction parallel to the cleavage planes. The length of a track is therefore independent of etching time, and one can select whichever etching time gives a convenient track diameter. This is normally ~0.5 to 1 $\mu$, which in muscovite mica corresponds to a time of ~10 min if concentrated (48%) HF at room temperature is used. If one is concerned only with track densities and not with track directions, a longer etching time of ~30 to 60 min will produce wide tracks which are easily viewable at 100×.

Both Lexan polycarbonate and cellulose nitrate are etched in a concentrated NaOH solution. In a 6.25 $N$ solution which is held at 55°C, the optimum etching times for producing the longest, narrowest tracks are ~50 min and 4 min, respectively. These conditions were used in the present work. Etching for longer times results in wide tracks which are more easily visible at low magnification.

[26] L. Voyvodic, Progr. Cos. Ray Phys. 2, 217 (1954).

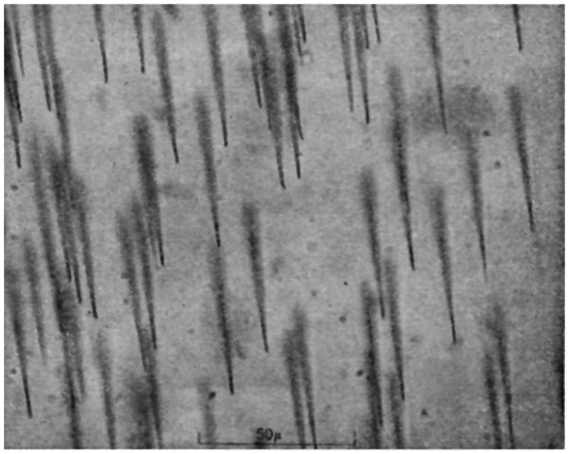


FIG. 4. Etched tracks of 139-MeV $S^{32}$ ions entering Lexan polycarbonate at a 30° angle. The average track length is $\sim 53\,\mu$, whereas the true range of the ions is estimated to be $60\,\mu$. The micrograph was taken by transmitted light with the microscope focused below the surface on the ends of the tracks.